2012

Phycoerythrin-Specific Bilin Lyase-Isomerase Controls Blue-Green Chromatic Acclimation in Marine Synechococcus

Wendy M. Schluchter
University of New Orleans, wschluch@uno.edu

Avijit Biswas
University of New Orleans, abiswas@uno.edu

Frédéric Partensky

J. A. Karty

Laurence Garczarek

See next page for additional authors

Recommended Citation

Shukla, A., Biswas, A., Blot, N., Partensky, F., Karty, J. A., Hammad, L. A., Garczarek, L., Gutu, A., Schluchter, W. M., & Kehoe, D. M. (2012). Phycoerythrin-specific bilin lyase-isomerase controls blue-green chromatic acclimation in marine Synechococcus. Proceedings of the National Academy of Sciences of the United States of America, 109(49), 20136–20141. (post print)

A phycoerythrin-specific bilin lyase-isomerase controls blue-green chromatic acclimation in marine *Synechococcus*

Animesh Shukla[a], Avijit Biswas[b], Nicolas Blot[c,d,e], Frédéric Partensky[c,d], Jonathan A. Karty[f], Loubna A. Hammad[f] , Laurence Garczarek[c,d], Andrian Gutu[a,g], Wendy M. Schluchter[b] and David M. Kehoe[a1]

[a]Department of Biology, Indiana University, Bloomington, Indiana, 47405 U.S.A.; [b]Department of Biological Sciences, University of New Orleans, New Orleans, Louisiana, 70148 U.S.A.; [c]UPMC-Université Paris 06, Station Biologique, 29680 Roscoff, France; [d]CNRS, UMR 7144 Adaptation et Diversité en Milieu Marin, Groupe Plancton Océanique, 29680 Roscoff, France; [e]Clermont Université, Université Blaise Pascal, UMR CNRS 6023, Laboratoire Microorganismes: Génome et Environnement, BP 10448, 63000 Clermont-Ferrand, France; [f]METACyt Biochemical Analysis Center, Department of Chemistry Indiana University, Bloomington, Indiana 47405 U.S.A.; [g]Howard Hughes Medical Institute, Department of Molecular and Cellular Biology, FAS Center for Systems Biology, Harvard University, Cambridge, Massachusetts, 02138, U.S.A.

Manuscript information: pages, 44; figures, 4; tables, 1; supplemental figures, 8; supplemental tables, 2.
The number of words in Abstract: 238 words
Total number of characters (with spaces) in manuscript: 52,067
Major category: Biological Science
Minor category: Plant Biology

Abbreviations: CA, chromatic acclimation; CA4, Type IV chromatic acclimation; CA3, Type III chromatic acclimation; GL, green light; BL, blue light; PBS, phycobilisomes; PC, phycocyanin; PE, phycoerythrin; PEI, phycoerythrin I; PEII, phycoerythrin II; PEB, phycoerythrobilin; PUB, phycourobilin; EIC, extracted ion chromatogram; MS, mass spectrometry

Keywords: bilin lyase; marine cyanobacteria; phycobilisomes; light regulation

[1]To whom correspondence should be addressed.
Department of Biology
1001 East 3rd Street
Indiana University
Bloomington, IN 47405 U.S.A.
E-mail: dkehoe@indiana.edu
Tel: (812) 856-4715
Fax: (812) 85-6705

Abstract

The marine cyanobacterium *Synechococcus* is the second most abundant phytoplanktonic organism in the world's oceans. Its ubiquity is in large part due to its use of a diverse set of photosynthetic light harvesting pigments called phycobiliproteins, which allow it to efficiently exploit a wide range of light colors. Here we uncover a pivotal molecular mechanism underpinning a widespread response among marine *Synechococcus* cells known as "Type IV chromatic acclimation" (CA4). During this process, the pigmentation of the two main phycobiliproteins of this organism, phycoerythrin I and II, is reversibly modified to match shifts in the ratio of ambient blue and green light so as to maximize photon capture for photosynthesis. CA4 involves the replacement of three molecules of the blue light-absorbing chromophore phycourobilin that are present in blue light with an equivalent number of the green light-absorbing chromophore phycoerythrobilin in green light. We have identified and characterized MpeZ, an enzyme critical for CA4 in marine *Synechococcus*. MpeZ attaches phycoerythrobilin to cysteine-83 of the alpha subunit of phycoerythrin II and isomerizes it to phycourobilin. *mpeZ* RNA is six times more abundant in blue light, suggesting that its proper regulation is critical for normal CA4, and *mpeZ* mutants fail to normally acclimate to blue light conditions. These findings provide insights into the molecular mechanisms controlling an ecologically important photosynthetic process and, since phycoerythrin is widely used in biotechnology, provide a new enzyme with potential for biotechnology and cell biology applications.

\body

Introduction

Synechococcus spp. cyanobacteria are found in marine environments from the equator to the polar circles and contribute significantly to the total phytoplankton biomass and productivity of the oceans (1-3). Their ubiquity is due in part to their wide pigment diversity (4), which mainly arises from differences in the composition of their light-harvesting antennae or phycobilisomes (PBS). PBS consist of a core and six or eight rods radiating from the core which contain the phycobiliproteins phycocyanin (PC) and one or two types of phycoerythrins (PEs), PEI and PEII (5). All phycobiliproteins are α/β heterodimers that are assembled into hexamers. PEs may bind two chromophores, green light (GL)-absorbing phycoerythrobilin (PEB) and blue light (BL)-absorbing phycourobilin (PUB). These chromophores are ligated to PE by PEB lyases (6, 7) or PEB-lyase-isomerases, which both attach the chromophore and isomerize it to PUB (8). No PE-specific PEB-lyase-isomerase has been described to date. PUB predominates in *Synechococcus* found in nutrient-poor open ocean waters, since blue photons penetrate the deepest in these vast areas (9). Four major marine *Synechococcus* pigment types do not change their chromophorylation profiles in response to shifts in ambient light color (4), although the size and numbers of their PBS may vary with irradiance (10). The fifth major *Synechococcus* pigment type, found in strains from different phylogenetic clades, varies its pigmentation in response to changes in ambient light color through a process called Type IV chromatic acclimation (hereafter CA4) (4, 11, 12).

Other CA types, such as CA2 and CA3, have been studied in freshwater cyanobacteria (13, 14). Like CA4, these processes are photoreversible, but they involve very different protein and bilin changes. For example, CA3 in *Fremyella diplosiphon*, which occurs when cells are shifted between red light and GL, involves switching between PC and PE and their corresponding chromophores in the rods of the PBS (14, 15). In contrast, CA4 occurs when marine *Synechococcus* cells are shifted between GL and BL, and during this process there is no change in the composition of PBS rods (11). Instead, CA4 was found to involve changes in the chromophores associated with two different cysteines within the α-PEII subunit (12). In GL, PEB is bound to these sites, whereas in BL, PUB is bound. The mechanism(s) controlling these changes is unknown. Here, we use biochemical and molecular genetic approaches to describe MpeZ, a novel enzyme involved in chromophore ligation and isomerization to PEII, and demonstrate its pivotal role in CA4.

Results

Comparative genomics analysis showed that all sequenced marine *Synechococcus* strains that undergo CA4 possess a specific gene, called *mpeZ* (4). In *Synechococcus* sp. RS9916 (hereafter 9916), *mpeZ* is downstream of a gene of unknown function and overlapping a gene putatively encoding a truncated form of the photosystem II core protein PsbA (Fig. 1*A*). RNA blot analysis demonstrated that *mpeZ* transcript accumulation was CA4 regulated, being six times more abundant in cells grown in BL than in GL (Fig. 1*B*). Primary and secondary structure analyses of the encoded protein, MpeZ, revealed a large domain belonging to the PBS lyase HEAT-like repeat family (Fig. S1), suggesting that

this protein could be a bilin lyase-isomerase involved in mediating the shift between PEB- and PUB-enriched PBS rods during CA4.

MpeZ was tested for lyase-isomerase activity by producing it in *Escherichia coli* cells expressing *ho1* and *pebS*, which encode the proteins needed for the synthesis of PEB (16), along with six-histidine tagged (HT) versions of wild type and mutant forms of either MpeA (PEII α subunit) or CpeA (PEI α subunit). Absorbance and fluorescence emission spectral analyses of purified wild type HT-MpeA from MpeZ-containing *E. coli* cells revealed absorbance and fluorescence maxima at 495 nm and 510 nm, respectively (Fig. 2*A*), which matched the spectral properties of PUB attached to protein (8, 17, 18). HT-MpeA was detectable on protein gels and contained an attached bilin (Fig. 2*C*). As expected, no absorbance or fluorescence was detectable from HT-MpeA expressed in cells lacking MpeZ (Fig. 2*A* and *C*), since non-chromophorylated recombinant PE subunits are generally insoluble in *E. coli* (6, 19). There are three canonical chromophore-binding cysteines at positions 75, 83, and 140 within MpeA. These cysteines were mutated to alanine in various combinations, and the constructs expressed in *E. coli* cells producing MpeZ and PEB. The spectral properties of purified HT-MpeA-C75A, C140A matched those of HT-MpeA, while HT-MpeA-C83A showed no absorbance or fluorescence, indicating that the latter form was non-chromophorylated (Fig. 2 *B* and *C*) (6, 19). When MpeZ was co-expressed with HT-CpeA in the PEB-producing *E. coli* strain, the HT-CpeA protein showed no absorbance or fluorescence, indicating that in this *E.coli* system, MpeZ does not chromophorylate CpeA (Fig. 2*B*). From these data we conclude that when expressed in *E. coli*, MpeZ functions as a

phycobilin lyase-isomerase, attaching PEB at Cys-83 of MpeA and isomerizing it to PUB (Fig. 2*D*).

To further analyze the role of MpeZ, we created an *mpeZ* insertion mutant in 9916 (Fig. S2) and tested it for its ability to carry out CA4 by recording the $Ex_{495\ nm}$: $Ex_{550\ nm}$ fluorescence excitation ratio, measuring emission at 580 nm (hereafter $Ex_{495:550}$), which has been used previously as a proxy for assessing the *in vivo* PUB:PEB ratio (12). For "control" cultures (cells with normal CA4, carrying the same antibiotic resistance marker as the *mpeZ* insertion mutant) acclimated to GL and then switched to BL, the $Ex_{495:550}$ shifted from 0.7 to 1.5 over a six day period and subsequently remained constant (Fig. 3*A*). In contrast, this ratio steadily rose from 0.7 to 0.9 for *mpeZ* cultures over the eleven day experimental period. Similar responses were obtained for control and *mpeZ* cultures when BL-acclimated cells were shifted to GL (Fig. 3*B*). Thus, the loss of MpeZ activity resulted in a 75% decrease in the $Ex_{495:550}$ in BL compared to the control, but had no obvious effect on this ratio in GL. Control and *mpeZ* cell growth was measured at three BL irradiances (Fig. 3*C*). Growth was similar for the two cultures at 15 μmol photons m^{-2} s^{-1} but was much slower in the mutant at 5 μmol photons m^{-2} s^{-1}. At 1 μmol photons m^{-2} s^{-1}, the control cells grew slowly while *mpeZ* cells showed virtually no growth. Thus, in BL, the disruption of *mpeZ* affected both the fluorescence characteristics of the PBS and growth, especially at low irradiances.

The PEI and PEII α and β subunits (CpeA, CpeB, MpeA and MpeB) were isolated from 9916 wild type and *mpeZ* cells grown in BL and GL (Fig. S3 *A* and *B*). The identity of

proteins in each of the major peaks was confirmed by mass spectrometry (MS). No difference was observed between the HPLC profiles of phycobiliproteins from wild type and *mpeZ* cells. Spectral analysis of isolated MpeA demonstrated that the absorption spectra were the same for wild type and the *mpeZ* mutant in GL but differed in BL, where PEB absorbance was detectable in the mutant but not in wild type cells (Fig. 3*D*). Similar analyses of isolated CpeA showed that the PUB:PEB absorbance ratios were the same in the wild type and *mpeZ* cultures in BL and GL (Fig. S3 *C* and *D*). These data demonstrate that MpeZ is involved in the attachment of PUB to MpeA, but not CpeA, in BL-grown wild type 9916 cells.

The type of bilins attached to the major PBS rod proteins of wild type and *mpeZ* mutant cells grown in BL and GL was determined using parallel ultraviolet-visible (UV-VIS) spectroscopy and tandem MS of HPLC-purified proteins. The MS peak intensities (extracted ion chromatograms, EICs) and UV-VIS spectra for MpeA-C83 tryptic peptides are provided in Fig. 4, while those for MpeA-C75 and MpeA-C140 tryptic peptides are provided in Fig. S4. Similar data for peptides containing CpeA-C82 and CpeA-C139 are presented in Figs. S5 and S6. The results for the HPLC purification and spectral analysis of CpeB and MpeB from wild type and the *mpeZ* mutant are shown in Fig. S7, while the UV-VIS spectra and MS peak intensities for tryptic peptides containing the four chromophore-binding cysteines of CpeB, the two chromophore-binding cysteines of MpeB, and the single chromophore-binding cysteine of RpcA, encoding the PC α subunit, are provided in Fig. S8. The data summarizing all of the analyses results is in Table 1, and show that CpeA-C139, MpeA-C83, and MpeA-C140 are the three amino

acids that have changes in bilin composition during CA4. In wild type cells, each has PEB attached in GL and PUB attached in BL, while in the *mpeZ* mutant MpeA-C83 fails to attach PUB in BL. These data demonstrate that the role of MpeZ in CA4 is to ligate PUB to MpeA-C83 during growth in BL.

Discussion

CA4 is a sophisticated physiological mechanism by which marine *Synechococcus* finely tunes the absorption properties of its antenna complexes to the ambient light color (4, 11). Here we show that MpeZ, present in all *Synechococcus* strains known to carry out CA4, is a key enzyme in this process. This enzyme is unique among phycobilin lyase-isomerases described so far because it chromophorylates phycoerythrin, specifically PEII. The only other such enzymes known are PecE/PecF, which bind phycocyanobilin at C84 of the phycoerythrocyanin α subunit and isomerize it to a phycoviolobilin (20) and RpcG, which ligates PEB at C84 of a phycocyanin α subunit and isomerizes it to PUB (8). All three enzymes belong to the E/F clan of phycobilin lyases, characterized by the presence of an α/α superhelix fold and Armadillo repeat motifs (21), although MpeZ is only distantly related to PecE/PecF and RpcG. It is particularly interesting that the conserved motif of PecF and the PecF-like C-terminus of RpcG that is involved in isomerization, NHCQGN, is absent in MpeZ (8, 22).

Our results are consistent with MpeZ's role in isomerization of PEB to PUB and its attachment at MpeA-C83 in BL. MS analyses revealed that the *mpeZ* mutant possesses a

PEB at MpeA-C83 in both BL and GL, indicating that PEB lyase activity is retained at this position. Though unlikely, we cannot rule out the possibility that the *mpeZ* mutant is producing a form of MpeZ that has kept its PEB binding activity but lost its isomerase activity. Recently, it was demonstrated that CpeY was involved in binding a PEB to CpeA-C82 from *Fremyella diplosiphon* (6) and that this reaction was facilitated by the presence of CpeZ. Since orthologs of CpeY/CpeZ are present in 9916, they very likely catalyze binding of PEB to CpeA-C82 and perhaps to MpeA-C83. Therefore, CpeY (+CpeZ)/MpeZ may be the lyase/lyase-isomerase set involved in the CA4-regulated change of chromophorylation at C83 on MpeA.

CA4-mediated changes in chromophorylation at the other two sites, CpeA-C139 and MpeA-C140 (Table 1), are likely mediated by one or two additional lyase/lyase-isomerase pair(s) that have not been identified yet. It is much less likely, but still formally possible, that a separate PUB synthesis pathway could exist that, in concert with the PEB synthesis pathway, increases the PUB:PEB ratio in BL and decreases it in GL.

An unexpected result from this study is that although MpeZ appears to be responsible for the chromophorylation of only one of the three sites that change chromophores during CA4, the $Ex_{495:550}$ dropped by 75% in the *mpeZ* mutant (Fig 3 *A* and *B*). This is a more dramatic decrease than might have been expected for a single chromophore change, but may be due in part to the position of the MpeA-C83 chromophore in the energy transfer flow within a PE hexamer. The structure of R-PE of *Polysiphonia urceolata* allowed distance measurements between bilins within a PE hexamer and estimates of likely

energy transfer pathways (23). PEB at CpeA-C83 played a critical role in transferring energy from the chromophores located on the outside of the PE hexamer (i.e.β50/61-PUB and α140-PEB in *P. urceolata*) to the terminal PEB acceptor located at β82 (5, 23). In 9916 cells grown in BL, the two external chromophores are β50/61-PUB and α140-PUB. In the *mpeZ* mutant, PEB at MpeA-C83 instead of the PUB in wild type cells (Table 1) may alter relaxation constraints within PEII and/or result in different spectral overlaps with the other bilins present within the hexamer, allowing for dissipation of the excited state by mechanisms other than fluorescence. Quantum yield and fluorescence lifetime measurements for PEII from BL-grown 9916 wild type and *mpeZ* cells should resolve this issue.

By allowing marine *Synechococcus* strains to alter their pigment ratios to match the ambient light color environment, CA4 is likely to confer a fitness advantage over those strains that have fixed pigmentation in habitats where the ratio of blue to green light varies frequently (4). Such an advantage appears to be conferred by CA3, which is beneficial in environments where the red to green light ratio varies over time periods longer than the CA3 acclimation time (24).

Given the remarkable ubiquity and abundance of marine *Synechococcus* in the world's oceans, CA4 must be a globally significant light color acclimation process. The discovery of the first lyase-isomerase controlling CA4 confirms previous proposals that such an enzyme(s) is critical for this response (4, 12). Two other forms of chromatic acclimation that have been analyzed, CA2 and CA3, are complex responses that involve changes in

the expression of genes encoding phycobiliprotein and bilin biosynthetic enzymes and lyases (6, 14). The fact that MpeZ is a PEII PEB lyase-isomerase, together with data showing that the composition of phycobiliproteins in the rods does not change during CA4 (12), demonstrates that CA4 is fundamentally different from other forms of CA. The development of CA4 appears to be an example of convergent evolution and is likely regulated through novel light sensing and signal transduction mechanisms (14).

The discovery of MpeZ provides a valuable addition to the array of phycobilin lyases available for producing natural or artificial phycobiliproteins for medical and biological research and industry (25, 26). Since PEB-containing PE conjugated to antibodies or other proteins is currently widely used in bioimaging and cell sorting applications due to its superior fluorescent properties, MpeZ will be a valuable tool for producing PUB-containing PE for *in vivo* biotechnological applications.

Materials and Methods

Strains and growth conditions. RS9916, isolated from 10 m depth in the Gulf of Aqaba (27), was obtained from the Roscoff Culture Collection (strain number RCC555) (4). Wild type or *mpeZ Synechococcus* RS9916 cells were grown at 22^{O}C in PCR-S11 (28) with or without 50 µg/ml kanamycin in polycarbonate Nalgene culture flasks in continuous light using Chroma75 T12 fluorescent bulbs (General Electric). Cultures were acclimated for at least seven days in BL or GL using filters (LE716 Mikkel Blue, LE738 Jas Green, Lee Filters, Burbank, CA) at 15 µmol photons m^{-2} s^{-1} unless noted.

Fluorescence excitation spectra were measured using a Biotek Synergy-Mx spectrofluorimeter and used to calculate the $Ex_{495:550}$.

Plasmid construction. Plasmids used are listed in Table S1 and primers used are listed in Table S2. pASmpeZ was made by PCR amplification of an ~800 nucleotide internal region of *mpeZ* using primers mpeZ-internal-for and mpeZ-internal-rev, cutting with BamHI and insertion into similarly cut pMUT100 (29). The cloning junctions and inserted *mpeZ* fragment were sequenced. One expression vector used was previously described (16). RS9916 *mpeA* and RS9916 *cpeA* were amplified using the corresponding primers listed in Table S2. Amplified fragments were cloned in the pCOLA-Duet (Novagen, Madison, WI) vector using BamHI-SalI to generate pCOLADuet-RS9916mpeA and into the BamHI and HindIII sites to create pCOLADuet-RS9916cpeA. RS9916 *mpeZ* was PCR amplified and cloned into BglII/XhoI cut pCDF-Duet (Novagen, Madison, WI) to create pCDF-RS9916mpeZ. The *mpeA* and *cpeA* sequences were inserted into pCOLADuet in-frame with the sequence encoding a HT. Single amino acid changes in *mpeA* were made using fusion PCR amplification and the primers listed in Table S2. All cloning junctions and PCR-amplified regions were sequenced.

***mpeZ* disruption.** pASmpeZ was transformed into *E. coli* MC1061 (30) containing pRK24 (31) and pRL528 (32). Bi-parental mating of exponentially growing RS9916 and *E. coli* cells was conducted as described (29), except that 9916 cells were grown in BL, then kept in darkness for two days before mating for a minimum of 72 h at 30^{O}C. Cells were plated as previously described (29), except that plates were kept at 22^{O}C at 5 μmol

photons m^{-2} s^{-1} for the first three days, then transferred to 15 µmol photons m^{-2} s^{-1}. Individual colonies were picked and tested for *mpeZ* disruption using PCR amplification, nucleotide sequencing and DNA blot analysis using a probe for *mpeZ*.

RNA analyses. One hundred ml of wild type 9916 cells at a density of approximately 10^9 cells ml^{-1} and grown in BL or GL were used for RNA analysis as previously described (33), using 10 µg/lane of RNA and a *mpeZ* probe radiolabelled as for the DNA blot.

Recombinant protein expression and purification. Expression plasmids were co-transformed into *E. coli* BL21 *DE3* cells and colonies were selected on Luria Bertani (LB) plates with the appropriate antibiotics as described in (6). To produce recombinant proteins, a single colony was inoculated into a 200-ml overnight culture in LB medium with the appropriate antibiotics and shaken at $20^{O}C$ at 180 rpm for 30-48 h until the optical density reached $OD_{600\ nm} = 0.6$. Production of T7 RNA polymerase was induced by the addition of 0.5 mM isopropyl β-D thiogalactoside (IPTG). Cells were incubated with shaking at 180 rpm at $20^{O}C$ for another 48 h before harvest by centrifugation. Cell pellets were immediately processed for protein purification as previously described (34). The entire purification process was carried out in the dark at $4^{O}C$. Following dialysis to remove imidazole, spectroscopic measurements were taken immediately.

Protein and bilin analysis. Polypeptides were resolved by SDS-PAGE (15% w/v) and polypeptides were visualized by staining with Coomassie Brilliant Blue R 250.

Fluorescence from bilins linked to proteins was detected with excitation at 488 nm as described in (6).

Fluorescence emission and absorbance spectra of purified proteins. Fluorescence emission and absorbance spectra were recorded as described in (6).

HPLC separation of phycobiliproteins. PBS were purified as described (35). HPLC was used to separate each phycobiliprotein as described in the legend for Fig S3. Fractions from the C4 column were collected for trypsin digestion, performed as previously described (6), and LC/MS/MS analyses.

Analysis of phycobiliproteins by LC/MS/MSLC/UV-VIS/MS: HPLC-separated and trypsin-digested phycobiliprotein samples from WT or *mpeZ* cells grown in BL or GL were separated by capillary HPLC as described in the legend for Fig S4. The UV-VIS detector recorded absorption spectra from 250-750 nm at 2.5 Hz. Tandem mass spectra were recorded and analyzed as described in the legend for Fig S4.

Acknowledgements

We thank the members of the Schluchter and Kehoe laboratories for thoughtful discussions and comments. This work was supported by grants to F.P. and L.G. from the French ANR program PELICAN (PCS-09-GENM-200) and the European program MicroB3 (EU-contract-287589), an International Projects and Activities Grant from the

Office of International Programs at Indiana University to D.M.K., and National Science Foundation Grants to D.M.K. (MCB-1029414) and to W.M.S. (MCB-0843664). The METACyt Biochemical Analysis Center was supported by a grant from the Lilly Foundation.

References

1. Olson RJ, Chisholm SW, Zettler ER, & Armbrust EV (1990) Pigments, size, and distribution of *Synechococcus* in the North Atlantic and Pacific Oceans. *Limnol Oceanogr* 35:45-58.
2. Partensky F, Blanchot J, & Vaulot D (1999) Differential distribution and ecology of *Prochlorococcus* and *Synechococcus* in oceanic waters: a review. *Marine Cyanobacteria*, eds Charpy L & Larkum A (Musée Océanographique, Monaco), Vol 19, pp 457-475.
3. Zwirglmaier K*, et al.* (2008) Global phylogeography of marine *Synechococcus* and *Prochlorococcus* reveals a distinct partitioning of lineages among oceanic biomes. *Environ Microbiol* 10:147-161.
4. Six C*, et al.* (2007) Diversity and evolution of phycobilisomes in marine *Synechococcus* spp.: a comparative genomics study. *Genome Biol* 8:R259.
5. Ong LJ & Glazer AN (1991) Phycoerythrins of marine unicellular cyanobacteria. 1. Bilin types and locations and energy-transfer pathways in *Synechococcus*-spp phycoerythrins. *J Biol Chem* 266:9515-9527.
6. Biswas A*, et al.* (2011) Characterization of the activities of the CpeY, CpeZ, and CpeS bilin lyases in phycoerythrin biosynthesis in *Fremyella diplosiphon* strain UTEX 481. *J Biol Chem* 286:35509–35521.
7. Wiethaus J*, et al.* (2010) CpeS is a lyase specific for attachment of 3Z-PEB to Cys(82) of beta-phycoerythrin from *Prochlorococcus marinus* MED4. *J Biol Chem* 285:37561-37569.
8. Blot N*, et al.* (2009) Phycourobilin in trichromatic phycocyanin from oceanic cyanobacteria is formed post-translationally by a phycoerythrobilin lyase-isomerase. *J Biol Chem* 284:9290-9298.
9. Morel A*, et al.* (2007) Optical properties of the "clearest" natural waters. *Limnol Oceanogr* 52:217-229.
10. Six C, Thomas JC, Brahamsha B, Lemoine Y, & Partensky F (2004) Photophysiology of the marine cyanobacterium *Synechococcus* sp. WH8102, a new model organism. *Aquat Micro Ecol* 35:17-29.
11. Palenik B (2001) Chromatic adaptation in marine *Synechococcus* strains. *Appl Environ Microbiol* 67:991-994.
12. Everroad C*, et al.* (2006) Biochemical bases of type IV chromatic adaptation in marine *Synechococcus* spp. *J Bacteriol* 188:3345-3356.

13. Tandeau de Marsac N (1983) Phycobilisomes and complementary chromatic adaptation in cyanobacteria. *Bulletin de l'Institut Pasteur* 81:201-254.
14. Gutu A & Kehoe DM (2012) Emerging perspectives on the mechanisms, regulation, and distribution of light color acclimation in cyanobacteria. *Mol Plant* 5:1-13.
15. Grossman AR (2003) A molecular understanding of complementary chromatic adaptation. *Photosynth Res* 76:207-215.
16. Dammeyer T, Bagby SC, Sullivan MB, Chisholm SW, & Frankenberg-Dinkel N (2008) Efficient phage-mediated pigment biosynthesis in oceanic cyanobacteria. *Current Biol* 18:442-448.
17. Glazer AN & Hixson CS (1977) Subunit structure and chromophore composition of rhodophytan phycoerythrins: *Porphyridium cruentum* B-phycoerythrin and b-phycoerythrin. *J Biol Chem* 252:32-42.
18. Bryant DA, Cohen-Bazire G, & Glazer AN (1981) Characterization of the biliproteins of *Gloeobacter violaceus*: chromophore content of a cyanobacterial phycoerythrin carrying phycourobilin chromophore. *Arch Microbiol* 129:190-198.
19. Fairchild CD & Glazer AN (1994) Nonenzymatic bilin addition to the α subunit of an apophycoerythrin. *J Biol Chem* 269:28988-28996.
20. Storf M*, et al.* (2001) Chromophore attachment to biliproteins: specificity of PecE/PecF, a lyase-isomerase for the photoactive 3(1)-Cys-alpha 84-phycoviolobilin chromophore of phycoerythrocyanin. *Biochem* 40:12444-12456.
21. Schluchter WM*, et al.* (2010) Phycobiliprotein biosynthesis in cyanobacteria: structure and function of enzymes involved in post-translational modification. *Adv Exp Med Biol* 675:211-228.
22. Zhao KH, Wu D, Zhou M, & Zhang L (2005) Amino acid residues associated with enzymatic activities of the isomerizing phycoviolobilin-lyase PecE/F. *Biochem* 44:8126-8137.
23. Jiang T, Zhang JP, & Liang DC (1999) Structure and function of chromophores in R-phycoerythrin at 1.9 angstrom resolution. *Proteins* 34:224-231.
24. Stomp M*, et al.* (2008) The timescale of phenotypic plasticity and its impact on competition in fluctuating environments. *Am Nat* 172:E169-E185.
25. Sekar S & Chandramohan M (2008) Phycobiliproteins as a commodity: trends in applied research, patents and commercialization. *J Appl Phycol* 20:113-136.
26. Glazer A (1994) Phycobiliproteins - a family of valuable, widely used fluorophores. *J Appl Phycol* 6:105-112.
27. Fuller NJ*, et al.* (2003) Clade-specific 16S ribosomal DNA oligonucleotides reveal the predominance of a single marine *Synechococcus* clade throughout a stratified water column in the Red Sea. *Appl Environ Microbiol* 69:2430-2443.
28. Rippka R*, et al.* (2000) *Prochlorococcus marinus* Chisholm et al. 1992 subsp. *pastoris* subsp. nov. strain PCC 9511, the first axenic chlorophyll a_2/b_2-containing cyanobacterium (Oxyphotobacteria). *Intl J Syst Evol Microbiol* 50:1833-1847.
29. Brahamsha B (1996) A genetic manipulation system for oceanic cyanobacteria of the genus *Synechococcus*. *Appl Environ Microbiol* 62:1747-1751.
30. Casadaban MJ & Cohen SN (1980) Analysis of gene control signals by DNA fusion and cloning in *Escherichia coli*. *J Mol Biol* 138:179-207.

31. Meyer R, Figurski D, & Helinski DR (1977) Physical and genetic studies with restriction endonucleases on broad host-range plasmid Rk2. *Mol Gen Genetics* 152:129-135.
32. Elhai J & Wolk CP (1988) Conjugal transfer of DNA to cyanobacteria. *Methods Enzymol* 167:747-754.
33. Seib LO & Kehoe DM (2002) A turquoise mutant genetically separates expression of genes encoding phycoerythrin and its associated linker peptides. *J Bacteriol* 184:962-970.
34. Shen G*, et al.* (2006) Identification and characterization of a new class of bilin lyase - the *cpcT* gene encodes a bilin lyase responsible for attachment of phycocyanobilin to Cys-153 on the beta-subunit of phycocyanin in *Synechococcus* sp PCC 7002. *J Biol Chem* 281:17768-17778.
35. Collier JL & Grossman AR (1992) Chlorosis induced by nutrient deprivation in *Synechococcus* sp Strain PCC 7942 - Not all bleaching is the same. *J Bacteriol* 174:4718-4726.
36. Dammeyer T, Hofmann E, & Frankenberg-Dinkel N (2008) Phycoerythrobilin synthase (PebS) of a marine virus - Crystal structures of the biliverdin complex and the substrate-free form. *J Biol Chem* 283:27547-27554.
37. Kelley LA & Sternberg MJE (2009) Protein structure prediction on the Web: a case study using the Phyre server. *Nature Protoc* 4:363-371.
38. Swanson RV & Glazer AN (1990) Separation of phycobiliprotein subunits by reverse-phase high-pressure liquid chromatography. *Anal Biochem* 188:295-299.
39. Perkins DN, Pappin DJC, Creasy DM, & Cottrell JS (1999) Probability-based protein identification by searching sequence databases using mass spectrometry data. *Electrophoresis* 20:3551-3567.
40. Shen GZ, Leonard HS, Schluchter WM, & Bryant DA (2008) CpcM posttranslationally methylates asparagine-71/72 of phycobiliprotein beta subunits in *Synechococcus* sp strain PCC 7002 and *Synechocystis* sp strain PCC 6803. *J Bacteriol* 190:4808-4817.
41. Bishop JE*, et al.* (1987) Chromopeptides from phycoerythrocyanin - Structure and linkage of the 3 bilin groups. *J Am Chem Soc* 109:875-881.
42. Schoenleber RW, Leung SL, Lundell DJ, Glazer AN, & Rapoport H (1983) Chromopeptides from phycoerythrins - Structure and linkage of a phycoerythrobilin tryptic tripeptide derived from a B-phycoerythrin. *Am Chem Soc* 105:4072-4076.
43. Nagy JO, Bishop JE, Klotz AV, Glazer AN, & Rapoport H (1985) Bilin attachment sites in the alpha-subunits, beta-subunits, and gamma-subunits of R-phycoerythrin - Structural studies on singly and doubly linked phycourobilins. *J Biol Chem* 260:4864-4868.

1

2

Table 1: Chromophores found at different cysteinyl sites for phycobiliproteins examined in the wild type (WT) and *mpeZ* cultures grown in BL and GL. The differences between BL and GL resulting from CA4 are highlighted in bold and the only difference between WT and mutant cells is underlined.

Protein	PUB:PEB ratio in GL	PUB:PEB ratio in BL	Cysteine position	Bilin in GL	Bilin in BL
CpeA-WT	2PEB	**1PUB:1PEB**	82	PEB	PEB
			139	**PEB**	**PUB**
MpeA-WT	1PUB:2PEB	**3PUB**	75	PUB	PUB
			83	**PEB**	**PUB**
			140	**PEB**	**PUB**
CpeB-WT	1PUB:2PEB	1PUB:2PEB	50, 61	PUB*	PUB*
			82	PEB	PEB*
			159	PEB*	PEB*
MpeB-WT	1PUB:2PEB	1PUB:2PEB	50, 61	PUB*	PUB*
			82	PEB	PEB*
			165	PEB*	PEB*
RpcA-WT			84	PUB	PUB
RpcB-WT			82	PCB	PCB
			153	PEB	PEB
MpeC-WT	1PUB	1PUB	49	PUB	PUB
CpeA-*mpeZ*⁻	2PEB	**1PUB:1PEB**	82	PEB	PEB
			139	**PEB**	**PUB**
MpeA-*mpeZ*⁻	1PUB:2PEB	**2PUB:1PEB**	75	PUB	PUB
			83	PEB	PEB
			140	**PEB**	**PUB**
CpeB-*mpeZ*⁻	1PUB:2PEB	1PUB:2PEB	50, 61	PUB*	PUB*
			82	PEB	PEB*
			159	PEB*	PEB*
MpeB-*mpeZ*⁻	1PUB:2PEB	1PUB:2PEB	50, 61	PUB*	PUB*
			82	PEB	PEB*
			165	PEB*	PEB*
RpcA-*mpeZ*⁻			84	PUB	PUB
RpcB-*mpeZ*⁻			82	PCB	PCB
			153	PEB	PEB
MpeC-*mpeZ*⁻	1PUB	1PUB	49	PUB	PUB

* These bilins were confirmed by LC-MS-MS (see Figure 4 and Supplemental Figures S4, S5, S5 ,and S8).

3

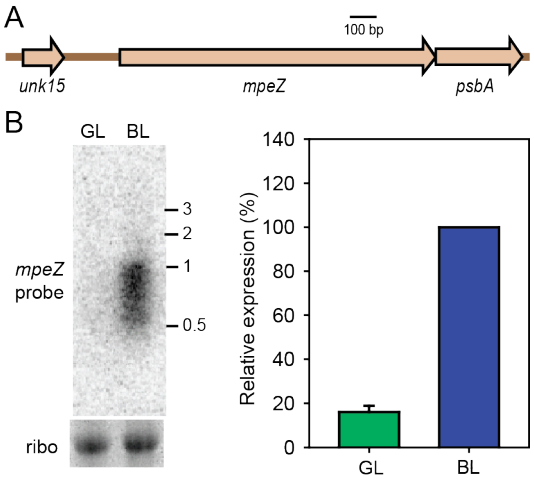

Figure 1. *mpeZ* genome localization and expression. (*A*) *mpeZ* genome context; "*psbA*" denotes a fragment of *psbA*. (*B*) Left, representative RNA blot of transcripts from cells acclimated to GL or BL using *mpeZ* and 16S rRNA (ribo) probes. Right, relative mean transcript levels of *mpeZ* in 9916 cells grown in GL or BL. Values expressed as a percent of transcripts from BL-grown cells after ribo normalization. Data are from three independent RNA blot analyses; error bars show SE.

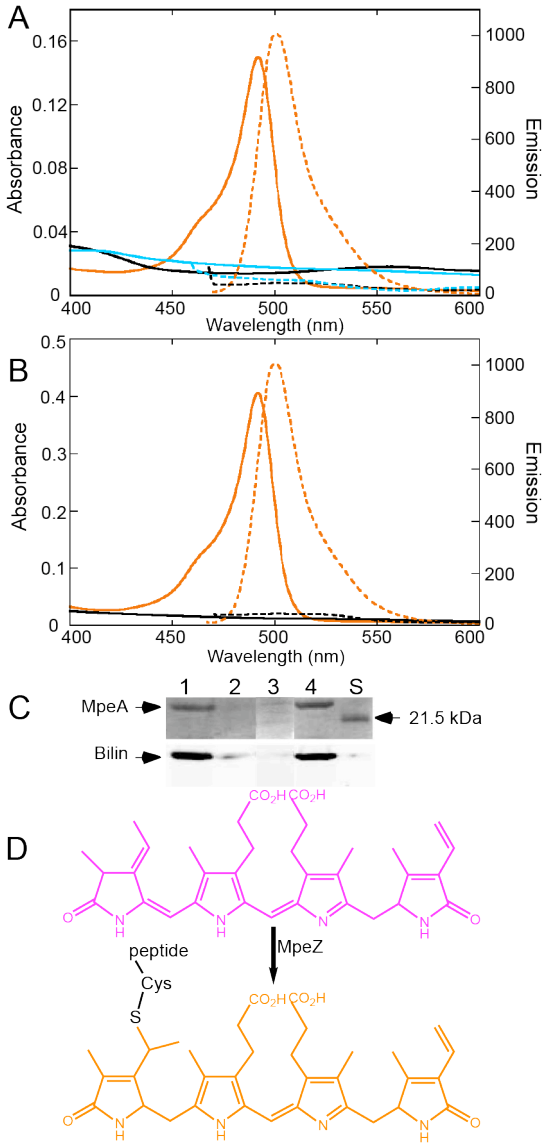

Figure 2. Analyses of recombinant HT-MpeA and HT-CpeA produced in presence or absence of MpeZ. (*A*) Absorbance (solid lines) and fluorescence emission (dashed lines) spectra for (i) HT-MpeA purified from cells containing MpeA, PEB (36) and MpeZ (orange) (ii) HT-MpeA purified from cells containing MpeA and PEB only (no MpeZ; black) and (iii) HT-CpeA purified from cells containing CpeA, PEB and MpeZ (aqua). (*B*) Absorbance (solid lines) and fluorescence emission (dashed lines) spectra for MpeA with cysteinyl binding sites replaced by alanines as (i) HT-MpeA-C75A,C140A purified from cells containing MpeA-C75A,C140A, PEB and MpeZ (orange) and (ii) HT-MpeA-

C83 purified from cells containing MpeA-C83A, PEB and MpeZ (black). (*C*) Upper panel, Coomassie-stained SDS polyacrylamide gel with HT-MpeA purified from cells containing MpeA, PEB with (lane 1) or without (lane 2) MpeZ, from cells with MpeA-C83A, PEB and MpeZ (lane 3) or from cells containing MpeA-C75A, C140A, PEB and MpeZ (lane 4). The molecular mass of the standard loaded in lane "S" is on right. Lower panel, zinc-enhanced fluorescence of bilins within the above gel. (*D*) The chemical reaction catalyzed by MpeZ is the attachment of PEB (pink) to an MpeA apoprotein (black) and its isomerization to PUB (orange).

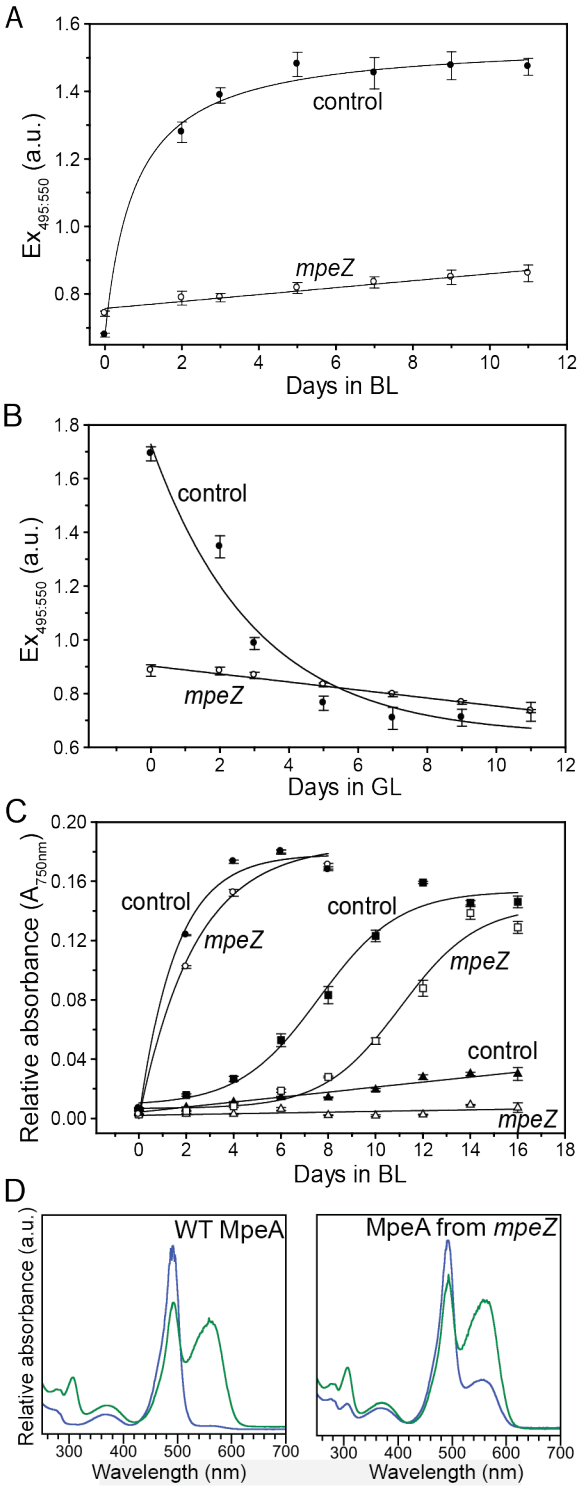

Figure 3. Effect of an *mpeZ* insertion on spectral properties and growth of 9916 cells. (*A*) $Ex_{495:550}$ from control (closed circles) and *mpeZ* mutant (open circles) cells grown in GL then shifted to BL at time zero. (*B*) $Ex_{495:550}$ from the same cell cultures grown in BL then

shifted to GL at time zero. (*C*) Growth curves for control (closed symbols) and *mpeZ* (open symbols) cells grown at different BL irradiances: circles, squares and triangles correspond to 15, 5, 1 μmol photons m^{-2} s^{-1}, respectively. (*D*) Absorption spectra of the MpeA protein purified from WT (left panel) or *mpeZ* mutant cells (right panel) grown in BL (blue line) and GL (green line).

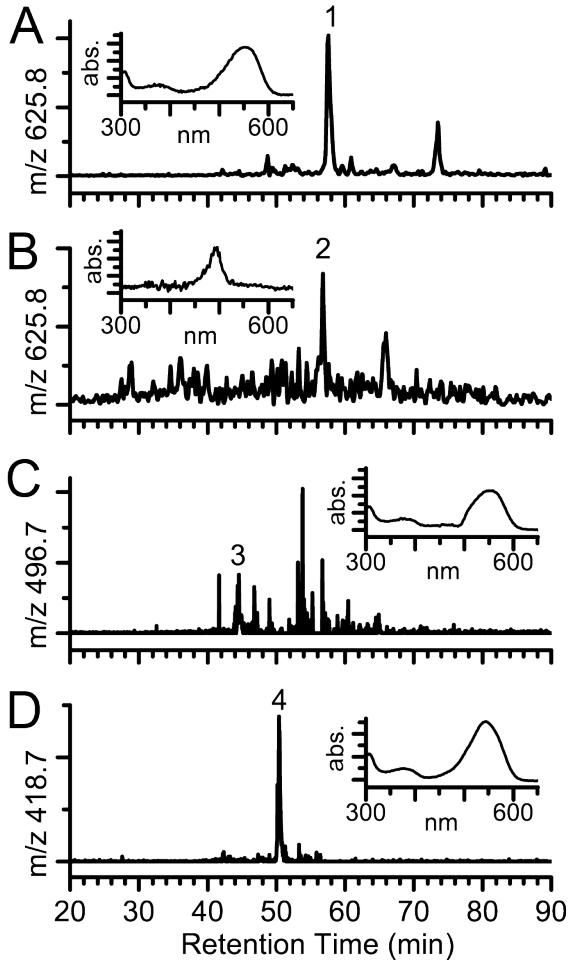

Figure 4. EICs and UV/VIS absorption spectra for tryptic peptides containing C83 of MpeA isolated from wild type (WT) 9916 and *mpeZ* mutant cells grown in BL or GL. (*A*) EIC for the peptide EKC*$_{83}$KR $(M+2H)^{2+}$ at m/z 625.8 (C* indicates that a bilin is attached to the cysteine) derived from WT cells grown in GL. Inset; UV/VIS absorption spectrum for the peak at retention time 57.5 min ("1" on the chromatogram) indicates PEB on C83. (*B*) EIC for the peptide EKC*$_{83}$KR $(M+2H)^{2+}$ at m/z 625.8 derived from BL-grown WT cells. Inset; UV/VIS absorption spectrum for the peak at 57.4 min ("2" on the chromatogram) indicates PUB on C83. (*C*) EIC for the peptide C*$_{83}$KR $(M+2H)^{2+}$ at

m/z 496.7 derived from GL-grown *mpeZ* cells. Inset; UV/VIS absorption spectrum for the peak at retention time 44.6 min ("3" on the chromatogram) indicates PEB on C83. (*D*) EIC for the peptide $C^*_{83}K$ $(M+2H)^{2+}$ at m/z 418.7 derived from BL-grown *mpeZ* cells. Inset; UV/VIS absorption spectrum at 50.0 min ("4" on the chromatogram) indicates PEB on C83.

Supporting Information

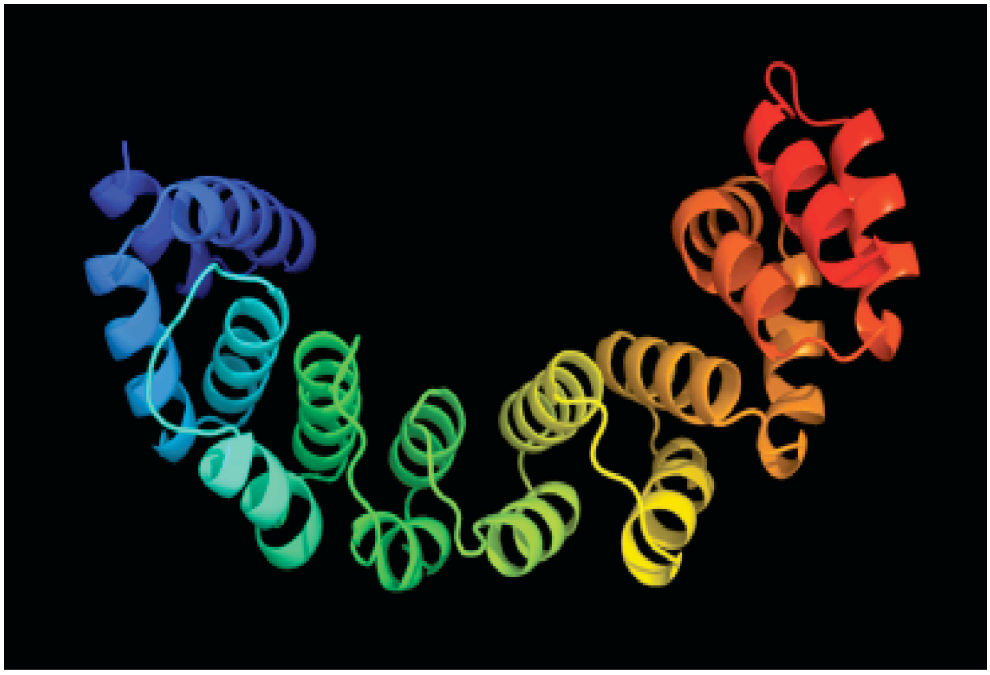

Figure S1. Analysis of the secondary structure of MpeZ using Phyre2 (37). 244 residues out of 413 (59% of MpeZ sequence) were modeled with 99.9% confidence to the PBS lyase HEAT-like repeat family by the single highest scoring template.

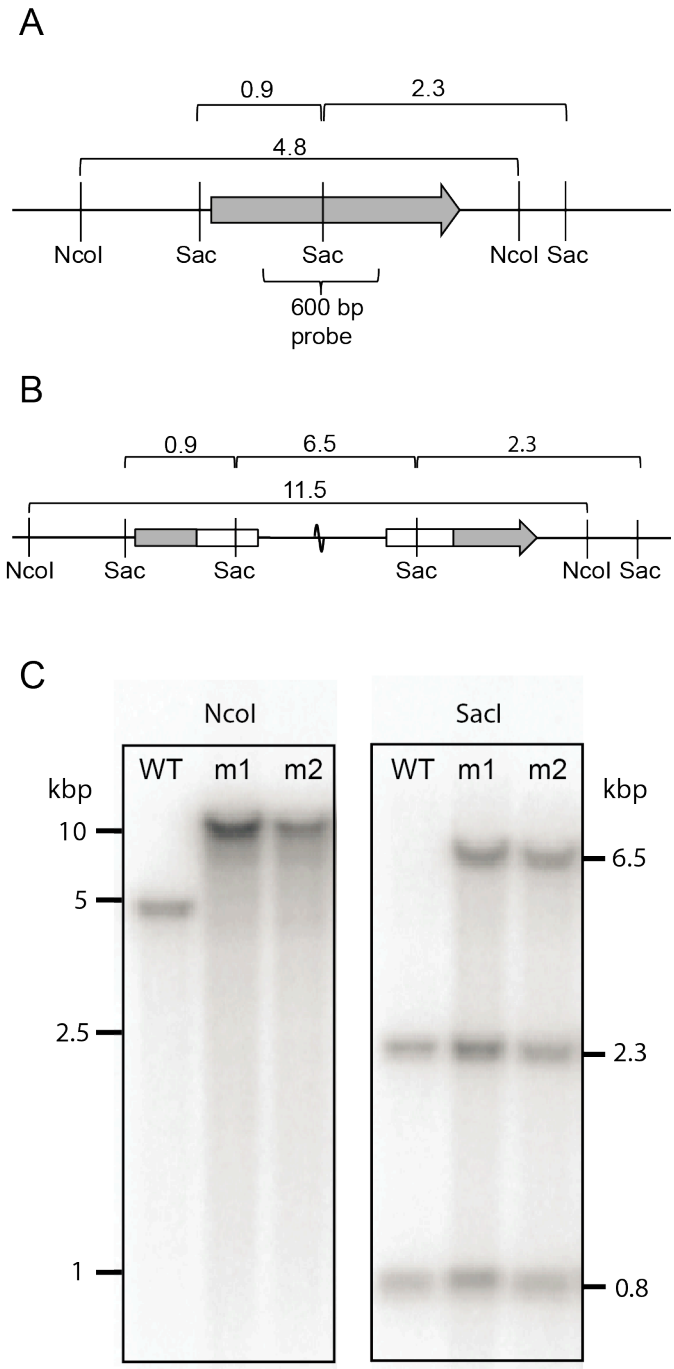

Figure S2. Restriction maps and DNA blot analysis show *mpeZ* disruption in two representative *mpeZ* mutants. (*A*) Restriction map of wild type 9916 (WT) at the *mpeZ* locus. (*B*) Restriction map of *mpeZ* mutant at the same locus. (*C*) DNA blot analysis of WT and two *mpeZ* insertion mutants using the 600 bp probe shown in *A*. Fifteen µg of

genomic DNA from 9916 wild type and putative *mpeZ* mutants were cut with NcoI and SacI for the analysis. Size markers are shown to the side of each blot.

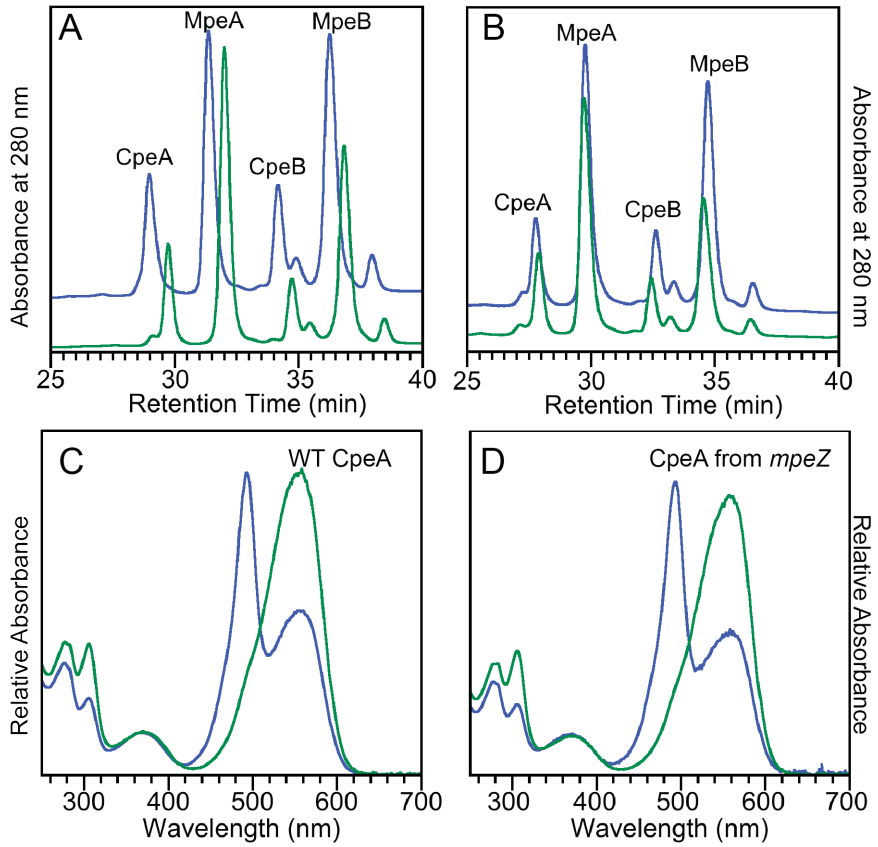

Figure S3. HPLC separation and spectral analysis of PUB/PEB chromophorylation patterns for the phycobiliproteins MpeA, MpeB, CpeA and CpeB. (*A*) The 280 nm chromatograms of wild type 9916 (WT) phycobiliproteins isolated in BL (blue line) and GL (green line) are shown offset. The identity of each protein as determined by mass spectrometry is labeled above each peak. (*B*) The 280 nm chromatograms of the *mpeZ* mutant phycobiliproteins isolated in BL (blue line) and GL (green line) are shown offset. The identity of each protein as determined by mass spectrometry is labeled above each peak. (*C*) Spectra of CpeA from WT cells grown in BL (blue line) and GL (green line). (*D*) Spectra of CpeA from *mpeZ* mutant cells grown in BL (blue line) and GL (green line). HPLC was performed using a Waters Delta 600 controller and Waters 2996

photodiode array detector (Waters Inc., Milford, MA). Prior to HPLC, PBS samples were dialyzed against 5 mM Na phosphate buffer, pH 7.0, concentrated, then combined (1:2 v/v) with 9 M urea, pH 2.0 for a final concentration of 6 M urea. This sample (~200 μl) was centrifuged prior to injecting on a C4 analytical column (250 x 4.6 mm: Hi-Pore® RP304 column; Bio-Rad, Richmond, CA) that was previously equilibrated in 65% Buffer A (0.1% trifluoroacetic acid (TFA; v/v in water) (buffer A), and 35% Buffer B (2:1 acetonitrile:isopropanol containing 0.1% TFA). The flow rate for the column was 1.5 ml min^{-1}. The linear gradient program used was as follows: 0-2 min, 65% buffer A, 35% buffer B; 2-37 min, 30% buffer A, 70% buffer B; 37-42 min, 100% buffer B; 42-47 min, 100% buffer B; 47-50 min, 65% buffer A, 35% buffer B; 50-55 min, 65% buffer A, 35% buffer B. This method was modified from one described earlier (38). Phycobiliproteins were monitored from 200-700 nm.

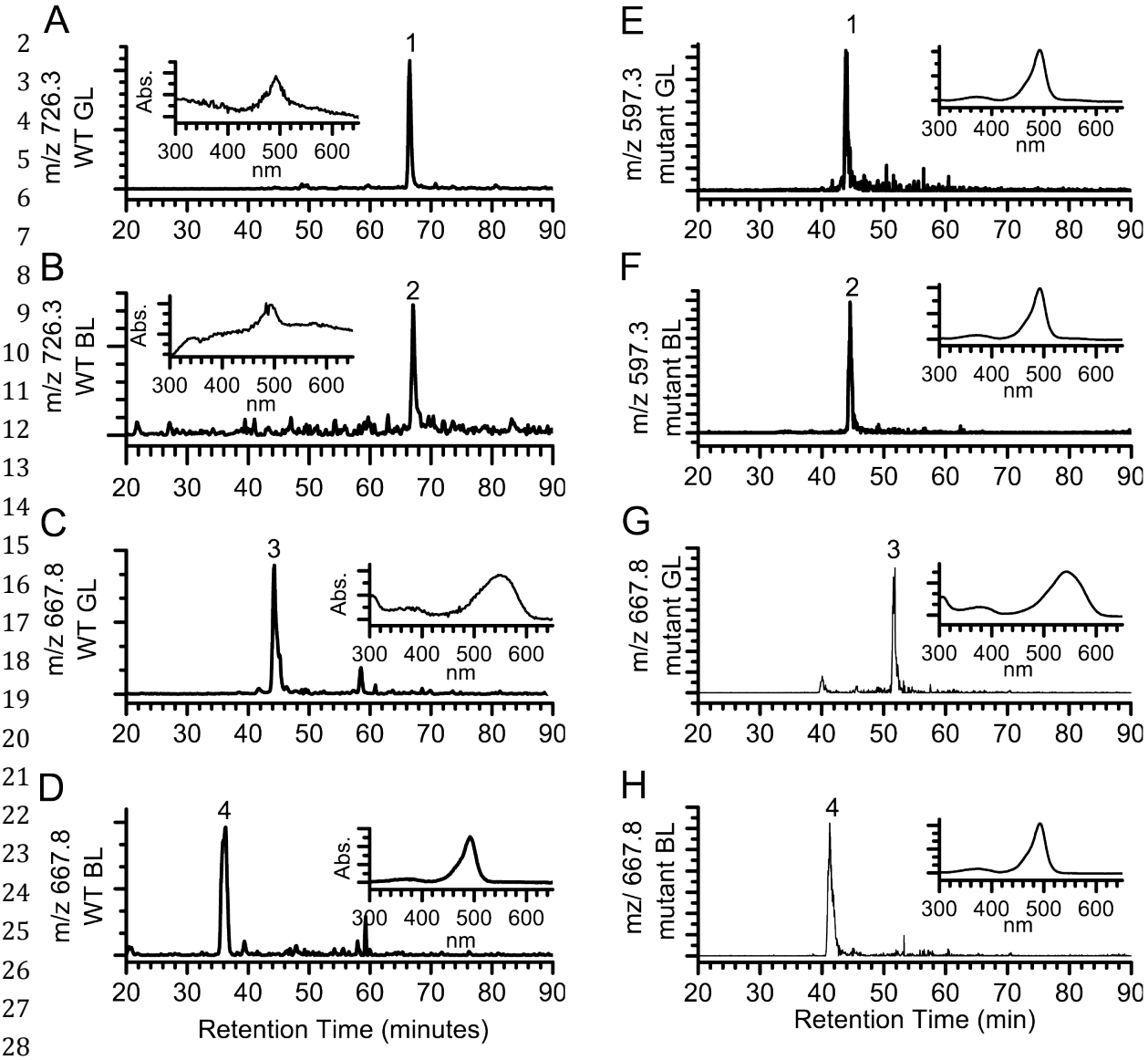

Figure S4. Extracted ion chromatograms (EICs) and UV-VIS absorption spectra for C75 and C140 of MpeA isolated from wild type 9916 (WT) or *mpeZ* mutant cells grown under various conditions. (*A*) EIC for KC*$_{75}$ATEGK $(M+2H)^{2+}$ at m/z 726.8 derived from WT cells grown in GL. The inset shows the UV-VIS spectrum at retention time 66.5 min ("1" on the chromatogram) and indicates C75 is modified by PUB. (*B*) The EIC

for KC*$_{75}$ATEGK isolated from WT cells grown in BL. The inset shows the UV-VIS spectrum at retention time 67.2 min ("2" on the chromatogram) and indicates PUB is the chromophore on C75. (*C*) EIC for NDGC*$_{140}$SPR $(M+2H)^{2+}$ at m/z 667.8 derived from WT cells grown in GL. The inset is the UV-VIS spectrum at retention time 44.3 min ("3" on the chromatogram) and suggests C140 is modified by PEB. (*D*) EIC for NDGC*$_{140}$SPR $(M+2H)^{2+}$ at m/z 667.8 derived from WT cells grown in BL. The UV-VIS spectrum from retention time 36.0 min ("4" on the chromatogram) suggests C140 is modified by PUB under these conditions. (*E*) EIC for C*$_{75}$ATEGK $(M+2H)^{2+}$ at m/z 597.3 derived from *mpeZ* mutant cells grown in GL. The inset shows the UV-VIS spectrum at retention time 44.0 min ("5" on the chromatogram) and indicates C75 is modified by PUB. (*F*) EIC for C*$_{75}$ATEGK $(M+2H)^{2+}$ at m/z 597.3 derived from *mpeZ* mutant cells grown in BL. The inset shows the UV-VIS spectrum at retention time 44.3 min ("6" on the chromatogram) and indicates C75 is modified by PUB. (*G*) EIC for NDGC*$_{140}$SPR $(M+2H)^{2+}$ at m/z 667.8 derived from *mpeZ* mutant cells grown in GL. The inset is the UV-VIS spectrum at retention time 51.5 min ("7" on the chromatogram) and suggests C140 is modified by PEB. (*H*) EIC for NDGC*$_{140}$SPR $(M+2H)^{2+}$ at m/z 667.8 derived from *mpeZ* mutant cells grown in BL. The UV-VIS spectrum from retention time 41.0 min ("8" on the chromatogram) suggests Cys_{140} is modified by PUB under these conditions. HPLC-separated and trypsin-digested phycobiliprotein samples from *mpeZ* cells grown in GL were reconstituted in 40 µl of LC-MS Buffer A prior to analysis (BL samples were reconstituted in 10 µl). LC-MS Buffer A was 97% v/v Omnisolve-grade water (EM-Science, Gibbstown, NJ), 3% v/v Omnisolve-grade acetonitrile (EM-Science), and 0.1% v/v formic acid (LC-MS grade, Fluka, St. Louis,

MO). LC-MS Buffer B was 97% v/v acetonitrile, 3% v/v water, and 0.1% v/v formic acid. The separation was performed with an Agilent 1200 capillary liquid chromatograph (Agilent Technologies, Santa Clara, CA) equipped with a diode array UV-VIS absorbance detector and a 500 nl flow cell. The column was 0.3 mm i.d., 150 mm long, and packed with 5 μm Zorbax SBC18-300 particles (Agilent). Three μl of each diluted sample were injected and the peptides separated at 4 μl/min with the following gradient: 5% B for 15 min, ramp to 55% B at 95 min, ramp to 85% B at 100 min, hold at 85% B for 10 min,, re-equilibrate the column at 5% B for 15 min (130 min total run time). The UV-VIS detector recorded absorption spectra from 250-750 nm at 2.5 Hz; chromatograms for 216 nm, 490 nm, 550 nm, and 620 nm (to detect all peptides, PUB, PEB, and PCB modified peptides, respectively) were also recorded. Tandem mass spectra were recorded in a data dependent fashion with a Bruker HCT-Ultra PTM ion trap mass spectrometer (Bruker Daltonics, Billerica, MA) placed after the diode array detector. Intact peptide mass spectra were recorded from m/z 400-1800 in "Standard Enhanced" mode. The three most intense ions in each spectrum were selected for collisionally induced dissociation (CID) tandem MS. Singly charged ions were not fragmented, and each precursor ion could only be selected three times prior to be placed on an exclusion list for 1.20 min. Peptide ions were activated using "SmartFrag" mode which ramped the activation energy from 0.4 to 2.0 V during the 40 msec fragmentation event; fragment mass spectra were recorded from m/z 200-1800 in UltraScan mode. Samples isolated from wild type cells were analyzed in a nearly identical fashion to the *mpeZ* mutant isolatesexcept that a 150 min HPLC gradient was employed.

The presence of each specific biliprotein was confirmed by comparing the tandem mass spectra to the *Synechococcus* RS9916 peptide FASTA file downloaded from the J. Craig Venter Institute website (https://moore.jcvi.org/moore/SingleOrganism.do?speciesTag=RS9916&pageAttr=pageMain) using MASCOT 2.2 (Matrix Science Inc. Boston, MA) (39). The search parameters were peptide mass error tolerance of ±1.2 Th, a fragment ion error tolerance of ±0.6 Th, +2 and +3 ions were preferred, and oxidation of methionine residues as well as modifications of cysteine by PEB/PUB (+586.27 Da) were considered. Bilin-containing peptides were confirmed manually using the following criteria: (i) the mass of the peptide had to match the predicted mass of a bilin-modified tryptic peptide (ii) a large fragment ion corresponding to the neutral loss of the bilin upon CID (M-586) and/or the presence of a significant fragment ion at m/z 587 (intact bilin+H^+) had to be observed (6, 40, 41). Finally, the UV-VIS absorption spectrum of the eluted peptide had to show an absorbance maximum at either 490 nm (for PUB) or 550 nm (for PEB).

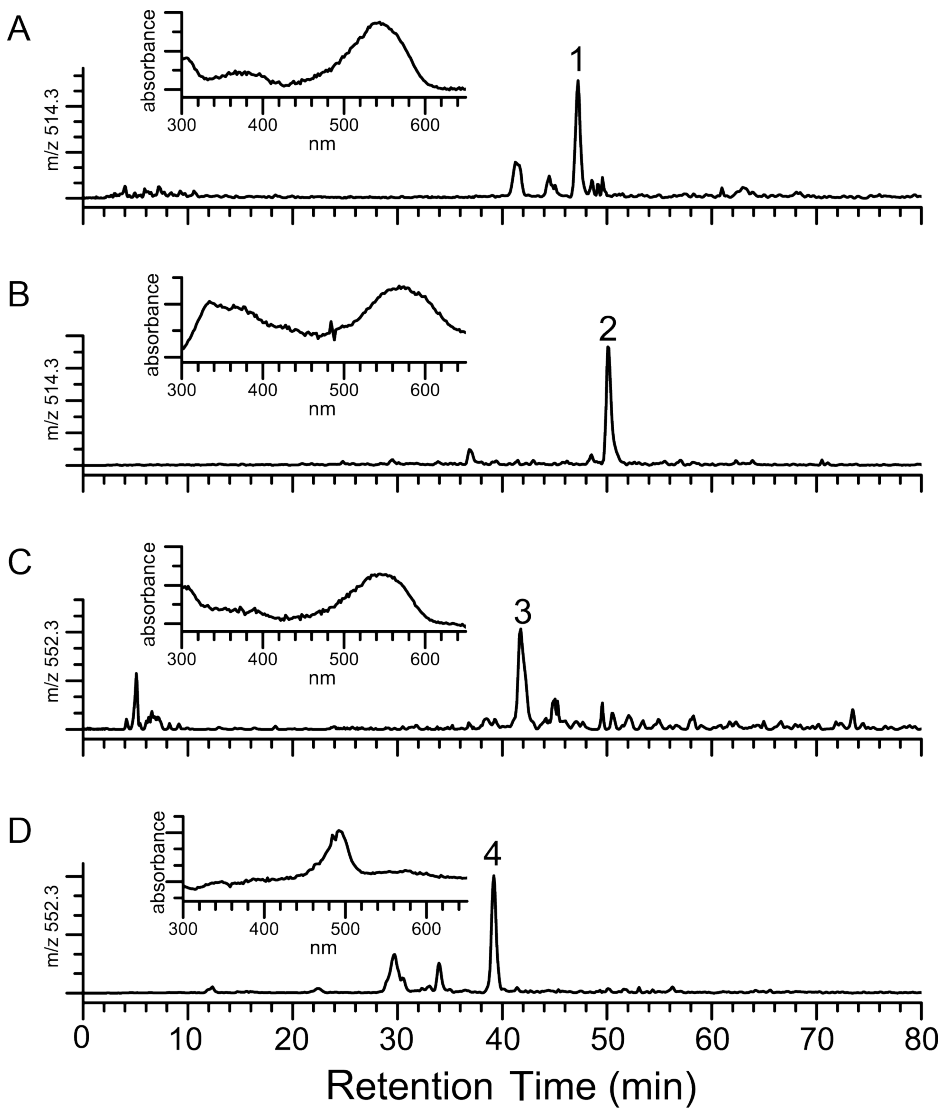

Figure S5. Extracted ion chromatograms (EICs) and UV-VIS spectra for tryptic peptides derived from CpeA isolated from wild type 9916 (WT) cells grown in GL and BL. (*A*) EIC for $C^*_{82}YR$ $(M+2H)^{2+}$ at m/z 514.3 derived from cells grown in GL. The inset shows the UV-VIS absorption spectrum at retention time 47.6 min ("1" on the chromatogram) and indicates C82 is modified by PEB. (*B*) EIC for $C^*_{82}YR$ $(M+2H)^{2+}$ at m/z 514.3 derived from cells grown in BL. The inset shows the UV-VIS absorption spectrum at retention time 50.1 min ("2" on the chromatogram) and indicates C82 is modified by

PEB. **(***C*) EIC for AC*$_{139}$APR $(M+2H)^{2+}$ at m/z 552.3 derived from cells grown in GL. The inset shows the UV-VIS absorption spectrum at retention time 42.0 min ("3" on the chromatogram) and indicates C139 is modified by PEB. (*D*) EIC for AC*$_{139}$APR $(M+2H)^{2+}$ at m/z 552.3 derived from cells grown in BL. The inset shows the UV-VIS absorption spectrum at retention time 39.2 min ("4" on the chromatogram) and indicates C139 is modified by PUB.

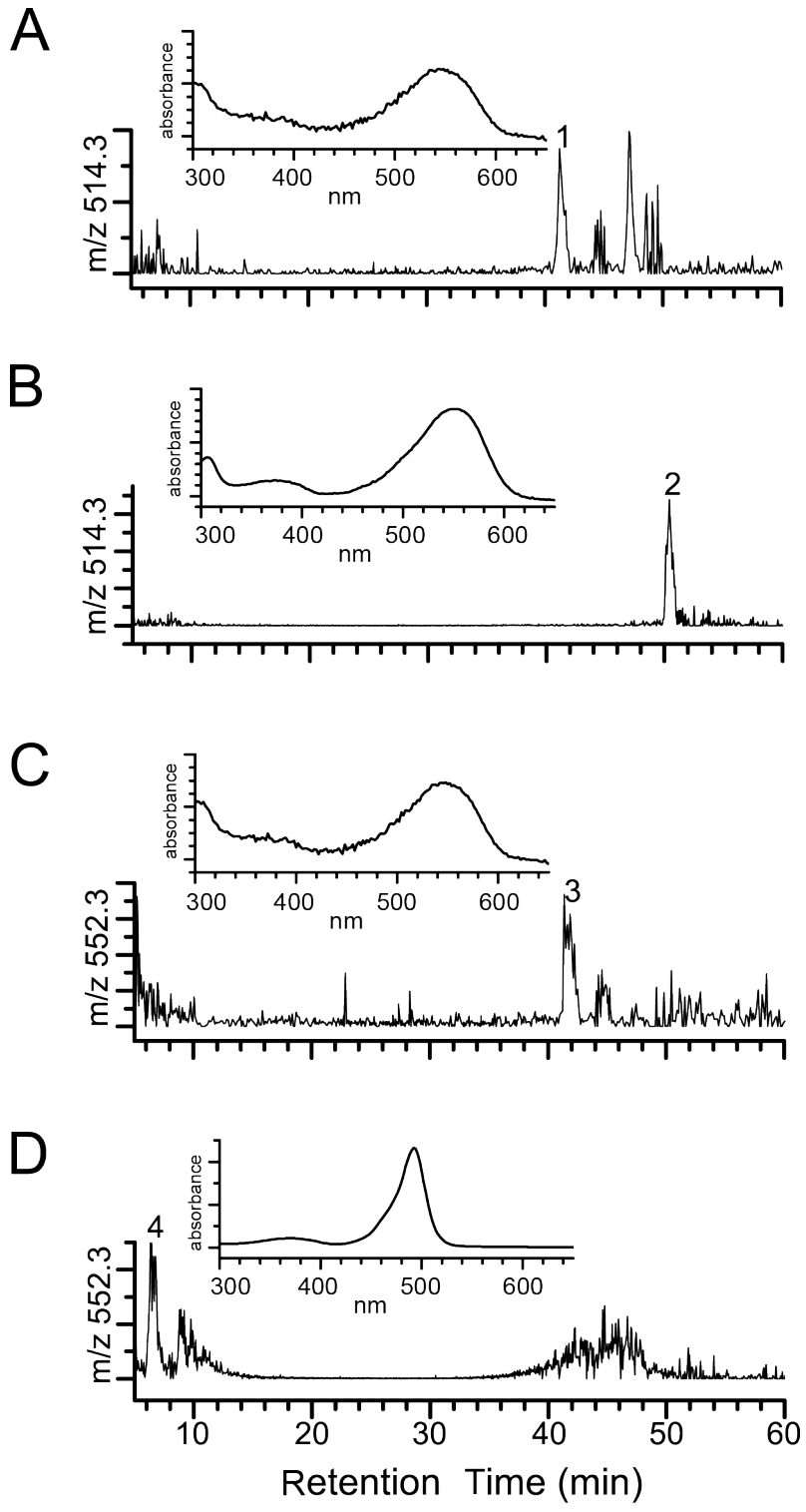

Figure S6. Extracted ion chromatograms (EICs) and UV-VIS spectra for tryptic peptides derived from CpeA isolated from *mpeZ* mutant cells grown in GL and BL. (*A*) EIC for

C*$_{82}$YR (M+2H)$^{2+}$ at m/z 514.3 derived from *mpeZ* cells grown in GL. The inset shows the UV-VIS absorption spectrum at retention time 41.6 min ("1" on the chromatogram) and indicates C82 is modified by PEB. (*B*) EIC for C*$_{82}$YR (M+2H)$^{2+}$ at m/z 514.3 derived from *mpeZ* cells grown in BL. The inset shows the UV-VIS absorption spectrum at retention time 50.1 min ("2" on the chromatogram) and indicates C82 is modified by PEB. **(***C*) EIC for AC*$_{139}$APR (M+2H)$^{2+}$ at m/z 552.3 derived from *mpeZ* cells grown in GL. The inset shows the UV-VIS absorption spectrum at retention time 41.5 min ("3" on the chromatogram) and indicates C139 is modified by PEB. (*D*) EIC for AC*$_{139}$APR (M+2H)$^{2+}$ at m/z 552.3 derived from *mpeZ* cells grown in BL. The inset shows the UV-VIS absorption spectrum at retention time 6.8 min ("4" on the chromatogram) and indicates C139 is modified by PUB.

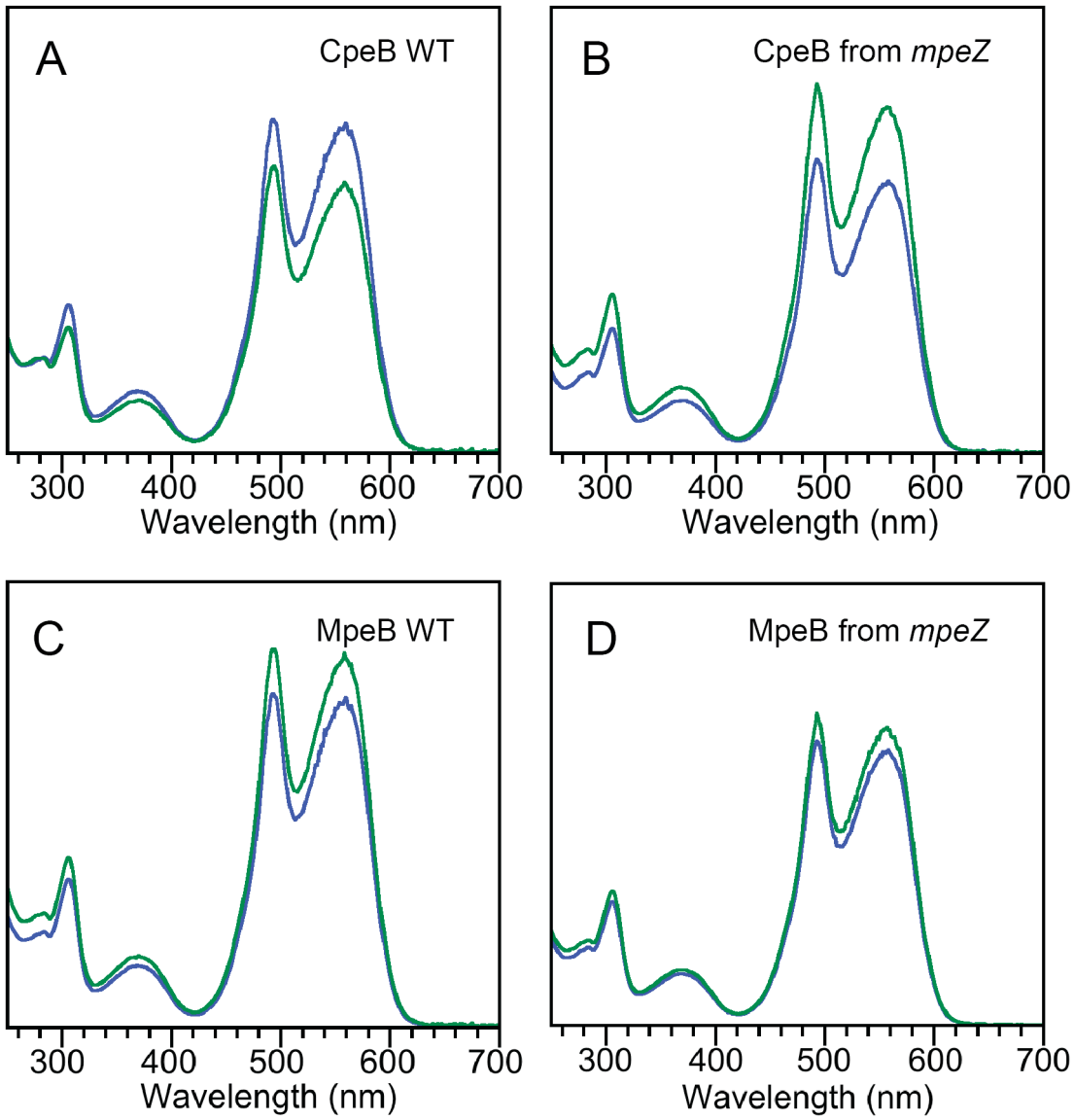

Figure S7. Spectral analyses of the PUB/PEB chromophorylation patterns for CpeB and MpeB after HPLC. (*A*) Spectra of CpeB (from the chromatogram shown in Fig. S3*A*) from wild type 9916 (WT) cells grown in BL (blue line) and GL (green line). (*B*) Spectra of CpeB from *mpeZ* cells (from the chromatogram shown in Fig. S3*B*). (*C*) Spectra of MpeB (from the chromatogram shown in Fig. S3*A*) from WT cells grown in BL (blue line) and GL (green line). (*D*) Spectra of MpeB from *mpeZ* cells (from the chromatogram shown in Fig. S3*B*).

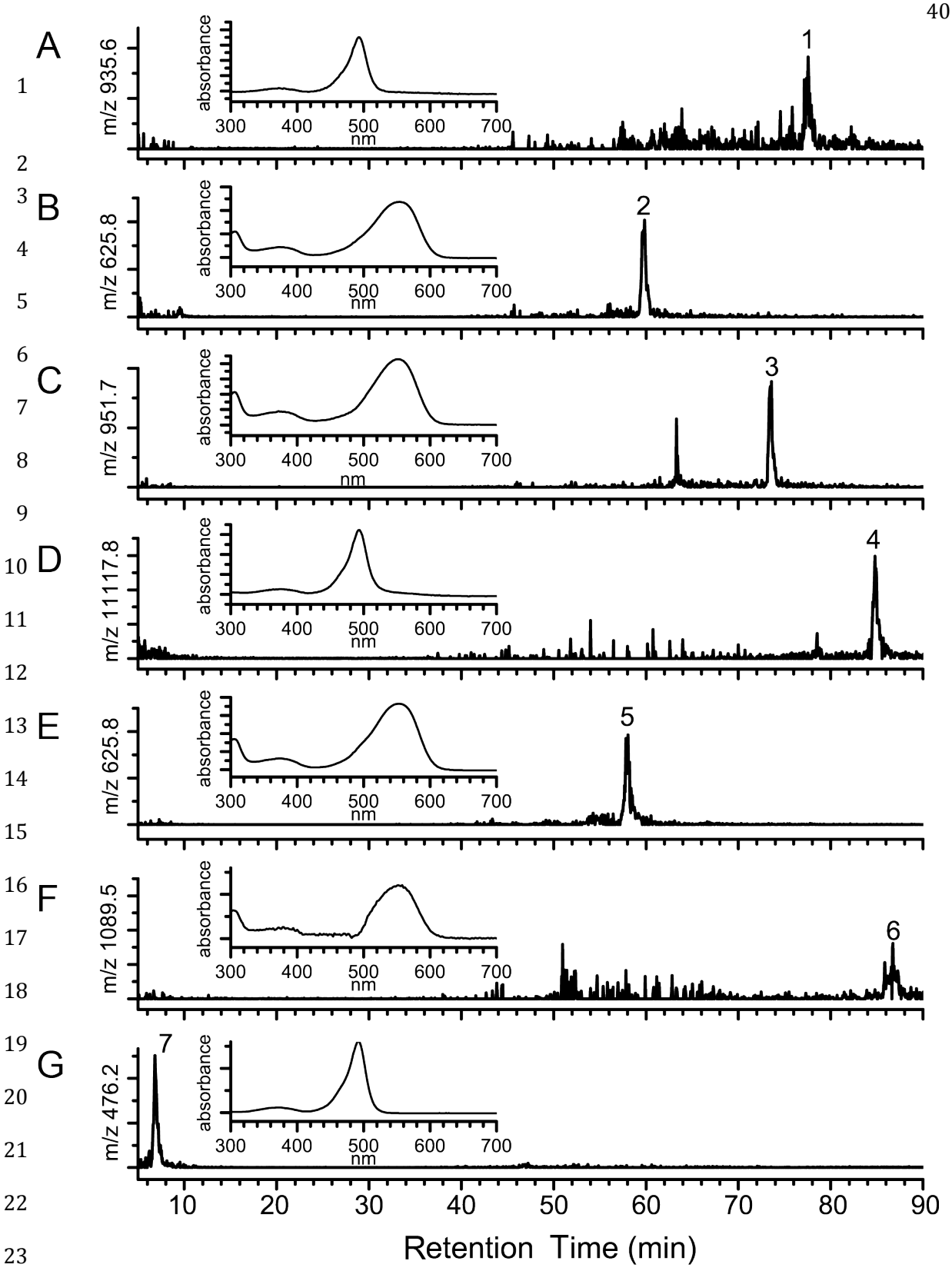

Figure S8. Extracted ion chromatograms (EICs) and UV-VIS absorption spectra for tryptic peptides of CpeB, MpeB, and RpcA isolated from a *mpeZ* mutant grown in GL.

(*A*) EIC for the peptide LDAVNAITSNASC$^{\dagger}_{50}$IVSDAVTGM$^{Ox}_{59}$IC$^{\dagger}_{61}$ENTGLIQAGGN$^{-CH3}_{72}$C$_{73}$YPNR $(M+5H)^{5+}$ from CpeB at m/z 935.8. Cys_{50} and Cys_{61} are expected to be cross-linked by a bilin (42, 43) as indicated by $C^{\dagger}$, Met_{59} is oxidized, and Asn_{72} is methylated (40); C73 is not modified. The inset shows the UV-VIS absorption spectrum at retention time 77.6 min ("1" on the chromatogram) and indicates PUB as the chromophore. (*B*) EIC for the peptide MAAC*$_{82}$LR $(M+2H)^{2+}$ from CpeB at m/z 625.8. The inset shows the UV-VIS absorption spectrum at retention time 59.4 min ("2" on the chromatogram) and indicates C82 is modified by PEB. (*C*) EIC for the peptide M$^{Ox}_{158}$ETTQGDC*$_{164}$SALVAEAGSYFDR $(M+3H)^{3+}$ from CpeB at m/z 951.7 (Met158 is oxidized). The inset shows the UV-VIS absorption spectrum at retention time 73.5 min ("3" on the chromatogram) and indicates C164 is modified by PEB. (*D*) EIC for the peptide LDAVNAIAGNAAC$^{\dagger}_{50}$IVSDAVAGIC$_{60}$C$^{\dagger}_{61}$ENTGLTAPNGGVYTNR $(M+4H)^{4+}$ from MpeB at m/z 1117.8. Cysteines 50 and 61 are expected to be cross-linked by a bilin (indicated by $C^{\dagger}$); cysteine 60 is not modified. The inset shows the UV-VIS spectrum at retention time 84.7 min ("4" on the chromatogram) and indicates the chromophore is PUB. (*E*) The EIC for peptide MAAC*$_{82}$LR $(M+2H)^{2+}$ from MpeB at m/z 625.8. The inset contains the UV-VIS spectrum at retention time 59.0 min ("5" on the chromatogram) and shows that C82 is modified by PEB. (*F*) EIC for the peptide AAVTQGDC*$_{159}$ASLSAEAGSYFDM$^{Ox}_{172}$VISAIS $(M+3H)^{3+}$ from MpeB at m/z 1089.5; Met_{172} is oxidized. The inset is the UV-VIS absorption spectrum at 86.1 min ("6" on the chromatogram) and shows C159 is modified by PEB. (*G*) EIC for C*$_{84}$SR $(M+2H)^{2+}$ from RpcA at m/z 476.2. The inset shows the UV-VIS spectrum at retention time 7.0 min ("7" on the chromatogram) and indicates PUB is the chromophore on C84.

Table S1. Plasmids used in this study

Plasmids	Relevant characteristics	Source
pColADuet-RS9916-mpeA	*mpeA* overexpression, N terminal His tag	This study
pColADuet-RS9916-mpeB	*mpeB* overexpression, N terminal His tag	This study
pColADuet-RS9916-cpeA	*cpeA* overexpression, N terminal His tag	This study
pCDFDuet-RS9916-mpeZ	*mpeZ* overexpression	This study
pPebS	phycoerythrobilin synthase overexpression	(16)
pCOLADuet-RS9916-mpeA-Cys83-Ala83	*mpeA* overexpression, Cys 83 mutated to Ala	This study
pCOLADuet-RS9916-mpeA-Cys140-Ala140	*mpeA* overexpression, Cys 140 mutated to Ala	This study
pCOLADuet-RS9916-mpeA-Cys75-Ala75	*mpeA* overexpression, Cys 75 mutated to Ala	This study
pCOLADuet-RS9916-mpeA-Cys83/140-Ala83/140	*mpeA* overexpression, Cys 83 & 140 mutated to Ala	This study
pCOLADuet-RS9916-mpeA-Cys75/140-Ala75/140	*mpeA* overexpression, Cys 75 & 140 mutated to Ala	This study
pCOLADuet-RS9916-mpeA-Cys75/83/140-Ala75/83/140	*mpeA* overexpression, Cys 75, 83 & 140 mutated to Ala	This study
pRL528	helper plasmid, carries *mob*	(32)
pRK24	conjugal plasmid, RK2 derivative	(31)
pMUT100	suicide vector backbone used for homologous recombination	(29)
pASmpeZ	*mpeZ* gene interruption, carries 1 kbp internal region of *mpeZ*	This study

Table S2. Primers used in this study

Primer	Sequence (5' to 3')
9916mpeAfor	tctcccttatgcgactcctgcatt
9916mpeArev	tgcggccgtgtacaatacgattac
9916mpeBfor	tctcccttatgcgactcctgcatt
9916mpeBrev	tgcggccgtgtacaatacgattac
9916mpeZfor	cggccgcataatgcttaagtcgaa
9916mpeZrev	actcgacagccaggaagaagtgaa
CpeA-BamHI-for	acgggatccaagtctgtcgtgaccaccgttgtg
CpeA-HindIII-rev	gcgaagctttcccctgaagctatgagcctctaa
mpeA-Cys83/140-Ala-for1	aaggagatataccatgggcagcagccat
mpeA-Cys83-Ala-rev1	acgcttggccttctctttgccttcggtggc
mpeA-Cys83-Ala-for2	aaagagaaggccaagcgtgacttcgttcac
mpeA-Cys140-Ala-rev1	tcatgtcgcgaggggaggcaccgtcgtta
mpeA-Cys140-Ala-for2	atgcgtaacgacggtgcctcccctcgcgaca
mpeA-Cys140-Ala-for2	taccagactcgagggtaccgacgt
mpeA-Cys75-Ala-for2	agcctcgtaaggccgccaccgaaggcaaa
mpeA-Cys75-Ala-rev1	tttgccttcggtggcggccttacgaggct
mpeZ-out-for1	aaggtcccagaggccatggccgcctt
mpeZ-trans-rev1	aagggcatcggtcgacgctctccctt
mpeZ-trans-for2	ttattgaagcatttatcagggttatt
mpeZ-out-rev2	ttgttagctttaggtttggatagcgtt
mpeZ-probe-for	agcctcatcacgatggctcagatt
mpeZ-probe-rev	aagatgccaaggctgtttctgctc
pMUT100-test-for	tcctgctcgcttcgctacttggagcca
pMUT100-test-rev	Actcctgcattaggaagcagcccagt